Downregulation of hepatic lipopolysaccharide binding protein improves lipogenesis-induced liver lipid accumulation

Jessica Latorre,[1,2,7] Ramon Díaz-Trelles,[3,7] Ferran Comas,[1,2] Aleix Gavaldà-Navarro,[2,4] Edward Milbank,[2,5] Nathalia Dragano,[2,5] Samantha Morón-Ros,[4] Rajesh Mukthavaram,[3] Francisco Ortega,[1,2] Anna Castells-Nobau,[1,2] Núria Oliveras-Cañellas,[1,2] Wifredo Ricart,[1,2] Priya P. Karmali,[3] Kiyoshi Tachikawa,[3] Pad Chivukula,[3] Francesc Villarroya,[2,4] Miguel López,[2,5] Marta Giralt,[2,4] José Manuel Fernández-Real,[1,2,6] and José María Moreno-Navarrete[1,2]

[1]Department of Diabetes, Endocrinology and Nutrition, Institut d'Investigació Biomèdica de Girona (IdIBGi), CIBEROBN (CB06/03/010) and Instituto de Salud Carlos III (ISCIII), 17007 Girona, Spain; [2]CIBER Fisiopatología de la Obesidad y Nutrición (CIBERobn), 28029, Madrid, Spain; [3]Arcturus Therapeutics, San Diego, CA 92121, USA; [4]Department of Biochemistry and Molecular Biomedicine, Faculty of Biology and Institute of Biomedicine (IBUB), University of Barcelona, CIBEROBN (CB06/03/025), 08028 Barcelona, Catalonia, Spain; [5]NeurObesity Group, Department of Physiology, CIMUS, University of Santiago de Compostela-Instituto de Investigación Sanitaria, 15782 Santiago de Compostela, Spain; [6]Department of Medicine, University of Girona, 17003 Girona, Spain

Circulating lipopolysaccharide-binding protein (LBP) is increased in individuals with liver steatosis. We aimed to evaluate the possible impact of liver LBP downregulation using lipid nanoparticle-containing chemically modified LBP small interfering RNA (siRNA) (LNP-*Lbp* UNA-siRNA) on the development of fatty liver. Weekly LNP-*Lbp* UNA-siRNA was administered to mice fed a standard chow diet, a high-fat and high-sucrose diet, and a methionine- and choline-deficient diet (MCD). In mice fed a high-fat and high-sucrose diet, which displayed induced liver lipogenesis, LBP downregulation led to reduced liver lipid accumulation, lipogenesis (mainly stearoyl-coenzyme A desaturase 1 [Scd1]) and lipid peroxidation-associated oxidative stress markers. LNP-*Lbp* UNA-siRNA also resulted in significantly decreased blood glucose levels during an insulin tolerance test. In mice fed a standard chow diet or an MCD, in which liver lipogenesis was not induced or was inhibited (especially *Scd1* mRNA), liver LBP downregulation did not impact on liver steatosis. The link between hepatocyte *LBP* and lipogenesis was further confirmed in palmitate-treated Hepa1-6 cells, in primary human hepatocytes, and in subjects with morbid obesity. Altogether, these data indicate that siRNA against liver *Lbp* mRNA constitutes a potential target therapy for obesity-associated fatty liver through the modulation of hepatic Scd1.

INTRODUCTION

Metabolic-associated fatty liver disease (MAFLD) is one of the main consequences of the overall burden of obesity worldwide[1–3] and contributes to aggravate other obesity-associated metabolic disturbances, such as insulin resistance, dyslipidemia, and type 2 diabetes, a common pathophysiology.[4]

In the last decade, circulating lipopolysaccharide binding protein (LBP) has been identified as a relevant component of innate immunity linked to obesity, insulin resistance and metabolic syndrome.[5–9] Circulating LBP has also been described to be associated with liver fat accumulation in children and adults.[10–13] Raised LBP seems to be causal because LBP KO mice fed a western style diet showed decreased liver steatosis.[14] The liver is the main source of circulating LBP,[15,16] being also present in adipose tissue.[17] To the best of our knowledge, the specific role of liver *LBP* in MAFLD has not been yet investigated.

Lipid-enabled and unlocked nucleic acid modified RNA (LUNAR®) is a safe, reproducible, and effective lipid nanoparticle (LNP) RNA delivery platform that specifically can be used to perform gene knockdown in liver.[18]

In the current study, we aimed to evaluate the specific impact of liver LBP knockdown in liver steatosis across the spectrum of fatness and explore the use of LBP as a therapeutic target using LUNAR technology. To that end, we studied the role of liver-specific LBP downregulation *in vivo* using different approaches to achieve liver steatosis, such as high-fat and high-sucrose diet and methionine- and choline-deficient diet (MCD). Given the scarcity of pharmacological therapies specific for MAFLD, the identification of new molecular targets is imperative.
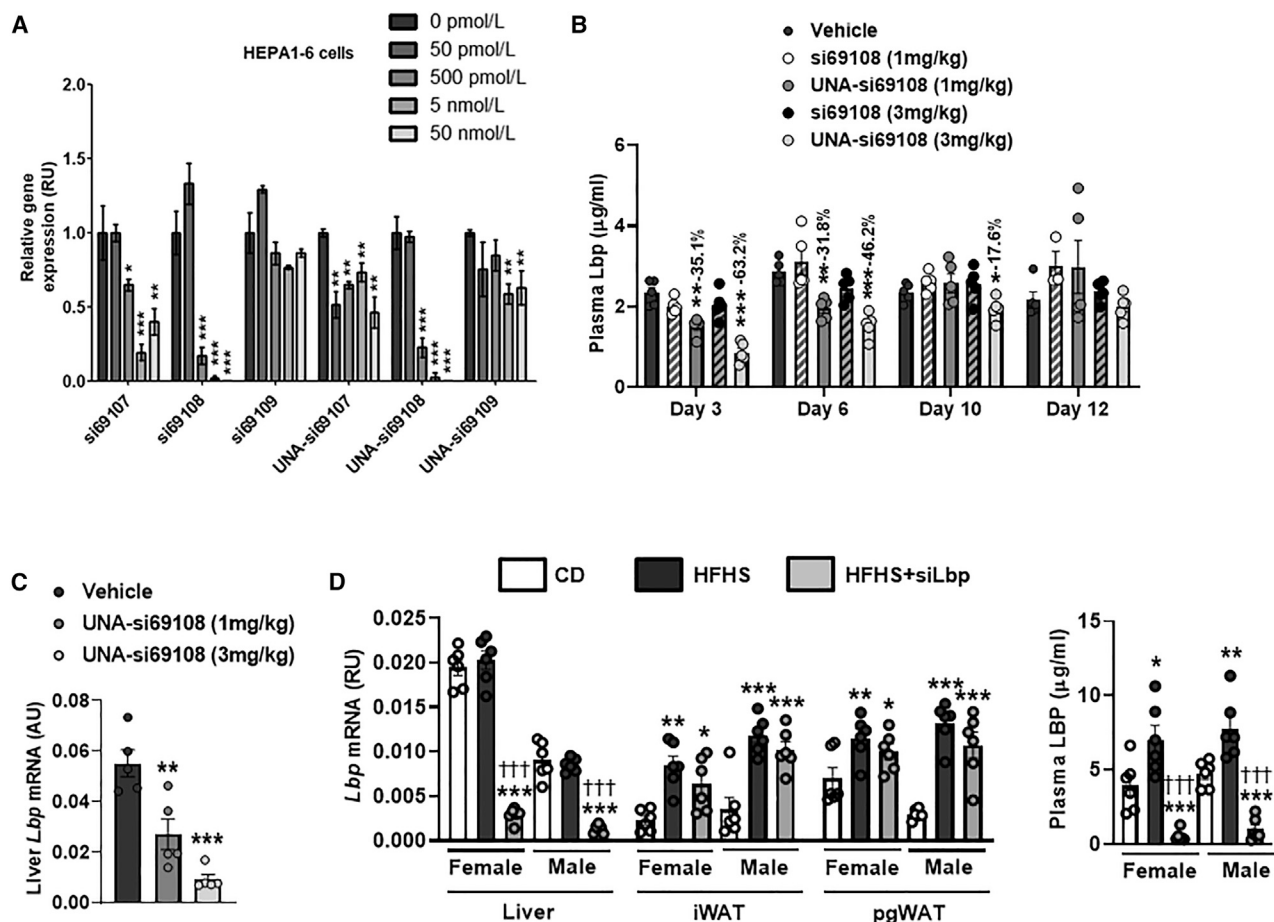
Figure 1. *In vitro* validation of Lbp siRNAs and *in vivo* effect of Lbp UNA-siRNA delivered through lipid nanoparticles

(A) Effect of several doses of chemically unmodified and modified (UNA) siRNA (si69107, si69108, si69109) against *Lbp* mRNA sequence in Hepa1-6 cell line. (B) Effect of chemically unmodified (1 and 3 mg/kg) and chemically modified (UNA, 1 and 3 mg/kg) LNP-*Lbp* siRNA on plasma LBP at days 3, 6, 10, and 12 after injection. (C) Effect of chemically modified (UNA, 1 and 3 mg/kg) LNP-*Lbp* siRNA on liver *Lbp* gene expression 3 days after second injection. *p < 0.05, **p < 0.01, and ***p < 0.001 compared with 0 pmol/L or vehicle. (D) Effects of 6-month LNP-*Lbp* UNA-siRNA administration in HFHS-fed mice on liver, inguinal WAT (iWAT), and perigonadal WAT (pgWAT) *Lbp* mRNA levels and plasma Lbp concentration in male and female mice. *p < 0.05, **p < 0.01, and ***p < 0.001 compared with CD; †p < 0.05, ††p < 0.01, and †††p < 0.001 compared with HFHS.

RESULTS

Lbp UNA-siRNA delivered through LNPs reduces liver *Lbp* gene expression and plasma LBP *in vivo*

To test *Lbp* siRNA efficacy *in vitro*, we screened three commercially available small interfering RNAs (siRNAs; si69107, si69108, si69109) at different doses in the Hepa1-6 cells. To increase siRNA stability and efficacy and to reduce the number of intravenous injections and potential immune response *in vivo*, we also tested the strategic introduction of chemical modifications in the three siRNAs. Both unmodified (si69108) and unlocked nucleomonomer agent (UNA)-containing chemically modified siRNA si69108 (UNA-si69108) sequences resulted in the most significant *Lbp* gene knockdown (Figure 1A) and were therefore selected for further *in vivo* studies, after being formulated in LUNAR LNPs (Arcturus Therapeutics), as detailed in the experimental procedures. This system has been

shown to deliver payloads specifically to the mouse hepatocytes.[18] Ten-week-old male mice were intravenously injected with vehicle (phosphate buffer saline), LUNAR with unmodified siRNA (LNP-si69108, 1 and 3 mg/kg), or LUNAR with chemically modified siRNA (LNP-UNA-si69108, 1 and 3 mg/kg). Three days after injection, plasma LBP levels were significantly decreased in the groups treated with LNP-UNA-si69108 but not in those treated with LNP-si69108 (Figure 1B), and this effect was maintained until day 6. At day 10, serum LBP levels were significantly lower only at the highest dose (3 mg/kg), returning to baseline levels 12 days after injection (Figure 1B). To confirm the dose-dependent inhibition of liver *Lbp* gene expression by LNP-UNA-si69108, a second intravenous injection was performed a week later in the same group of mice, at 1 and 3 mg/kg, and the mice were sacrificed after 3 days. Liver *Lbp* gene-expression analysis confirmed the dose-dependent inhibition
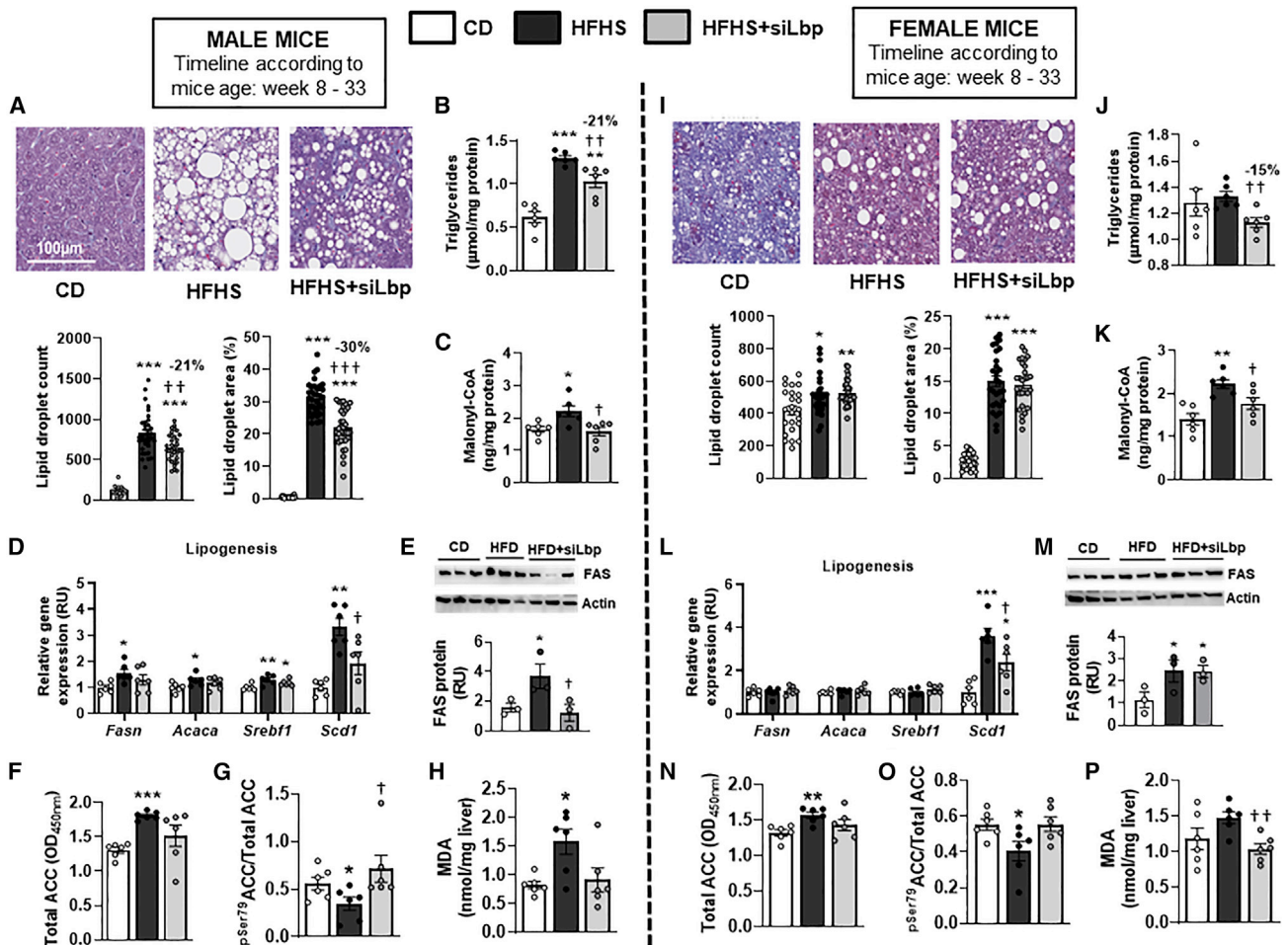
Figure 2. Effect of LNP-*Lbp* UNA-siRNA treatment on liver lipid accumulation and lipogenesis induced by an HFHS diet

(A–P) Effects of 6-months LNP-*Lbp* UNA-siRNA administration on representative standard Masson's trichrome staining histological liver slides (20×), lipid droplet (LD) count and area (A and I), liver triglycerides (B and J), malonyl-CoA levels (C and K), expression of lipogenic (D and L) genes, FAS and ACC protein (E, F, M, and N), ACC activity (G and O), and MDA levels (H and P) in HFHS-fed male (A–H) and female (I–P) mice. *$p < 0.05$, **$p < 0.01$, and ***$p < 0.001$ compared with CD; [†]$p < 0.05$, [††]$p < 0.01$, and [†††]$p < 0.001$ compared with HFHS.

of liver *Lbp* mRNA levels by LNP-UNA-si69108 (Figure 1C). Considering the data from this *in vivo* pilot experiment and to avoid side effects that may arise using higher doses, the dose of 3 mg/kg was selected for the following experiments.

Delivery of LNP-*Lbp* UNA-siRNA prevents liver lipid accumulation and lipogenesis induced by high-fat and high-sucrose diet
We first evaluated whether the treatment of mice with LNP-UNA-si69108 could prevent lipid accumulation in the liver under obesogenic conditions. To set up this mouse model, mice were fed a high-fat and high-sucrose diet (HFHS) to promote liver steatosis (Figures S1A–S1C).[19]

Diet effect
In both males and females, HFHS-induced obesity did not significantly change liver *Lbp* mRNA levels (Figure 1D). In males, an

HFHS resulted in a significant increased hepatic lipid accumulation (Figures 2 and S2), including lipid droplet count and area (Figure 2A) and triglycerides (Figure 2B) and signs of liver damage, such as increased hepatocyte vacuolation (with a histopathology score ranging between 4 and 5), serum alanine transaminase (ALT) levels, and expression of some inflammatory markers (*Itgax* and *Ccl2* mRNA) (Figures S2A–S2C). Liver *Lbp* mRNA was increased by 2-fold in females compared with males fed a control diet or an HFHS (Figure 1D). In line with this increased liver *Lbp* mRNA levels in females, liver lipid droplet counts and area, liver triglycerides, and hepatocyte vacuolation were all higher in female mice versus males fed a standard diet (Figures 2I, 2J, and S2F). In sharp contrast, the increase in lipid accumulation, ALT, and liver *Itgax* and *Ccl2* mRNA levels in mice fed an HFHS diet was lower in females versus males (Figures 2I, 2J, and S2F–S2H). These data confirmed the resistance of females to the adverse effects of an HFHS diet.[20] HFHS increased some markers of

lipogenesis and oxidative stress-related genes (including *Scd1*, *Gsta3*, and *Gpx4* mRNA, malonyl-coenzyme A [CoA], FAS, total ACC protein, and ACC activity) in females (Figures 2K–O and S2J).

Effects of LBP downregulation

LNP-UNA-si69108 significantly decreased liver *Lbp* mRNA levels in males fed an HFHS diet (84.6%, p < 0.0001) (Figure 1D), in parallel to decreased liver lipid droplet count and area, liver triglycerides, and a trend to decreased hepatocyte vacuolation (Figures 2A, 2B, and S2A) without significant effects on serum ALT levels or gene expression related to liver inflammation/liver damage (Figures S2B and S2C). Markers of liver lipogenesis (such as malonyl-CoA levels, *Fasn*, *Acaca*, *Scd1*, and *Srebf1* gene expression, FAS protein, total ACC levels, and ACC activity [reduced phosphorylation of Ser79 in ACC]) were all significantly increased in HFHS-fed male mice and were significantly prevented by LNP-UNA-si69108 administration (Figures 2C–2G). This intervention also prevented an increased expression of genes related to NADPH production (isocitrate dehydrogenase 1 [*Idh1*] and cytosolic malic enzyme [*Me1*]) (Figure S2D), which also are important to sustain liver lipogenesis,[21–23] and attenuated oxidative stress markers induced by lipid peroxidation (*Gsta3*, *Gpx4*, and *Sod2* mRNA and malondialdehyde [MDA] levels) (Figures 2H and S2E). In females, LNP-UNA-si69108 administration also decreased liver *Lbp* mRNA levels (85.7%, p < 0.0001) (Figure 1D), liver triglycerides (Figure 2J), *Scd1* mRNA, malonyl-CoA, and MDA levels and attenuated the increase in ACC protein and activity (increased [phosphoSer79]ACC/total ACC ratio indicates reduced ACC activity) (Figures 2K, 2L, and 2N–2P).

These data indicate that weekly LNP-UNA-si69108 treatment for 6 months is efficacious in reducing lipid accumulation, without significant changes in liver damage (Figures S2A–S2C and S2F–S2H) or body weight (Figure S3A), compared with HFHS control mice.

LNP-*Lbp* UNA-siRNA treatment reduces liver lipid accumulation and lipogenesis in mice with established obesity

After observing that *Lbp* UNA-siRNA prevented lipid accumulation in mice fed an HFHS diet, we evaluated whether this therapy could reduce liver fat accumulation in mice with obesity induced by an HFHS diet, in which liver lipogenesis (*Scd1* mRNA) was also induced. Once the mice reached a plateau of increased fat mass, weekly *Lbp* UNA-siRNA administration was initiated and maintained for 8 weeks (Figures S1D, S3B, and 3). This intervention in obese animals also led to reduced liver *Lbp* mRNA levels and parallel decreased liver lipid accumulation (lipid droplet count and area and triglycerides) both in males (Figures 3A–3C) and females (Figures 3I–3K). We also observed decreased hepatocyte vacuolation in females, with a non-significant decrease in fibrosis score and ALT levels both in males and females, without any effects on expression of liver inflammation/liver damage-related genes (except for a significant reduction in *Il6* mRNA levels in males) (Figure S4). Again, *Lbp* UNA-siRNA also resulted in decreased lipogenic pathway, significantly reducing *Fasn*, *Acaca*, *Scd1*, *Srefb1* mRNA, malonyl-CoA, and ACC protein in males (Figures 3D–3G) and *Acaca*, *Scd1* mRNA, malonyl-CoA, and ACC activity in females (Figures 3L–3O). Liver MDA levels,

Idh1 and *Me1* (in both sexes), and *Gpx4* and *Sod2* mRNAs (in males) also decreased significantly (Figures 3H, 3P, S4D, S4E, S4I, and S4J).

These experiments confirmed that *Lbp* UNA-siRNA administration is effective in liver fat reduction in an obesity and insulin-resistance context, where the lipogenic pathway has been induced, through the specific inhibition of this pathway.

LNP-*Lbp* UNA-siRNA improves insulin action in HFHS-fed mice and in mice with established obesity

During development of HFHS-induced obesity, we observed increased insulin levels at weeks 4 and 8 in male compared with female mice (Figure 4A) and also in HFHS compared with control diet (CD) at week 8 but only in males (Figure 4A). Of note, LNP-UNA-si69108 treatment significantly reduced insulin increase from weeks 4 to 8 in male mice (Figure 4B). In addition, fasting glucose and homeostatic model assessment for insulin resistance (HOMA$_{IR}$) were also significantly increased in male compared with female mice (Figures 4C and 4D). LNP-UNA-si69108 intervention decreased HOMA$_{IR}$ (Figure 4D) and improved insulin sensitivity during an insulin tolerance test (ITT) in males. This effect was not observed in females (Figures 4E and 4F).

In line with this, in mice with established obesity treated with LNP-UNA-si69108 for 8 weeks, glycemia was reduced at 30, 45, and 90 min in males and at 60 and 90 min in females, and glycemia area under the curve (AUC) was improved during ITT (Figures 4G and 4H). Similar to the previous experiment, when male and female mice were compared, impaired ITTs in male mice were found (Figures 4G and 4H).

Thus, females were more resistant to the metabolic derangement induced by HFHS, with LNP-*Lbp* UNA-siRNA able to improve insulin action in insulin-resistant male mice.

LNP-non-targeting UNA-siRNA did not impact on liver parameters

To discriminate off-target effects of LNP UNA-siRNA, the impact of 6-week LNP-non-targeting UNA-siRNA administration on Lbp and liver parameters was assayed. No significant differences on liver *Lbp* gene expression and serum LBP levels, neither on liver triglycerides, lipogenesis, and markers of oxidative stress, inflammation, and liver damage, were found in mice treated with LNP-non-targeting UNA-siRNA (3 mg/kg) compared with vehicle (Figure S5). These results indicated that changes on the different liver parameters were not related to the repeated dosing of the LUNAR LNPs but were specific to the *Lbp* knockdown.

LNP-*Lbp* UNA-siRNA requires the induction of hepatic *Scd1* to impact on liver lipid accumulation

Current data point to the attenuation of HFHS-induced liver lipogenesis after LBP downregulation. We next studied whether the latter could also target non-alcoholic steatohepatitis (NASH) in another established mice model, the MCD[24] (Figure 5). Under the MCD, weekly LNP-UNA-si69108 administration blunted liver *Lbp* mRNA
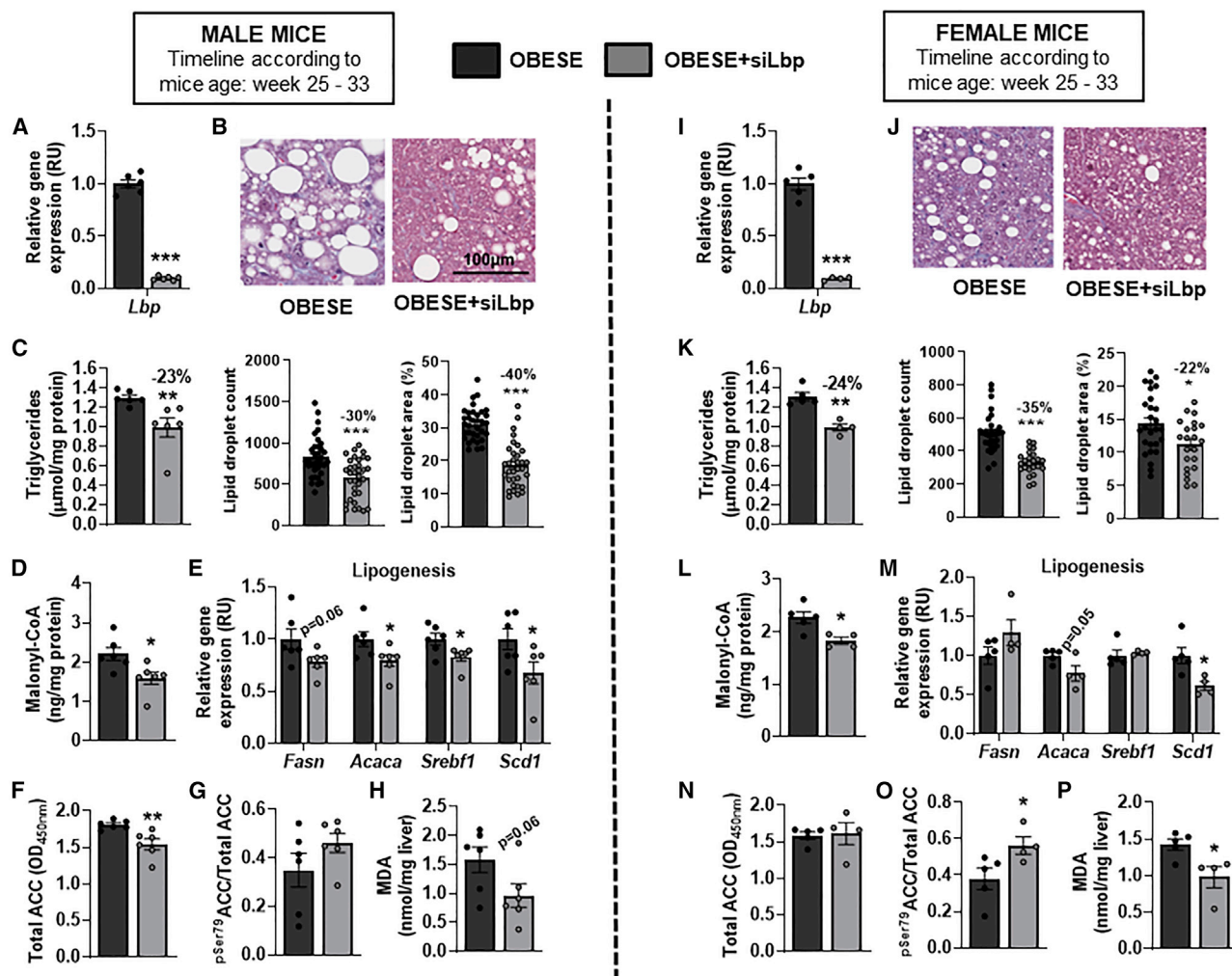
Figure 3. Result of LNP-*Lbp* UNA-siRNA treatment on liver lipid accumulation and lipogenesis in mice with established obesity
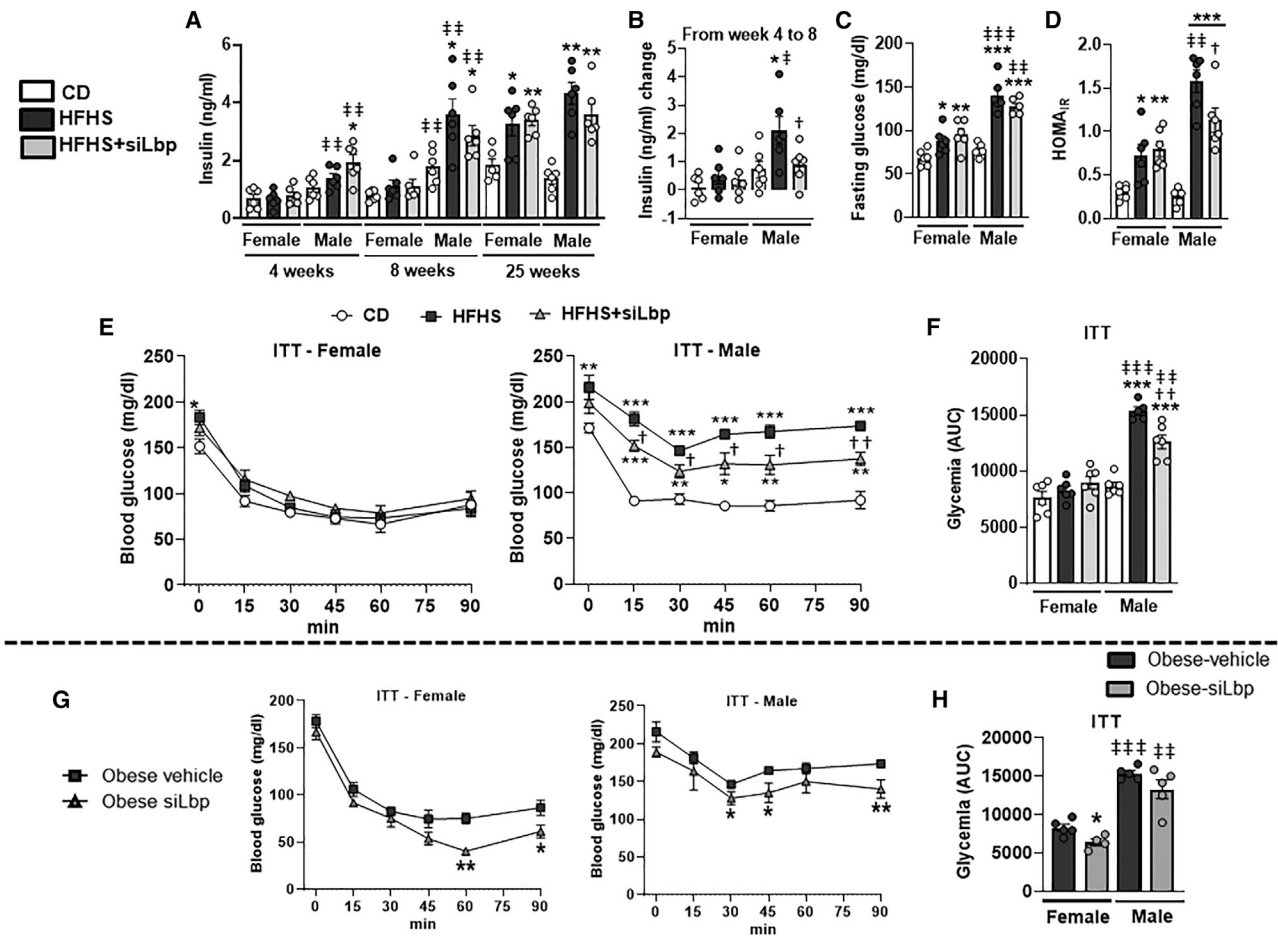
(A–P) Effects of 8-weeks LNP-*Lbp* UNA-siRNA administration on *Lbp* mRNA levels (A and I), representative standard Masson's trichrome staining histological liver slides (20×), LD count and area (B and J), liver triglycerides (C and K), malonyl-CoA levels (D and L), expression of lipogenic (E and M) genes, ACC protein (F and N), ACC activity (G and O), and MDA levels (H and P) in diet-induced obese male (A–H) and female (I–P) mice. *p < 0.05, **p < 0.01, and ***p < 0.001 compared with vehicle-treated obese mice.

(Figure 5A). In this model, *Scd1* mRNA was markedly suppressed (Figure 5B). Surprisingly, Lbp downregulation did not impact liver lipogenesis (Figures 5B–5G), MDA (Figure 5H), or liver triglycerides levels (Figure 5I). These data suggest that LBP knockdown prevents the worsening of liver steatosis only when liver lipogenesis/Scd1 has been previously triggered.

Lbp gene knockdown attenuated the detrimental effects of palmitate in murine hepatoma cell line

To gain insight in the potential mechanisms that underlie the positive effects of Lbp depletion on liver metabolism, *in vitro* experiments were performed in the murine Hepa1-6 cell line after palmitate versus vehicle (bovine serum albumin [BSA]). *Lbp* gene knockdown was performed using lentiviral particles with Lbp-specific short hairpin RNA (shRNA) (Figure 6A). In normal conditions (BSA), *Lbp* gene knock-

down led to decreased *Scd1*, *Me1*, *Gpx4*, and *Sod2*, without significant effects on ACC and AMPK activity (Figures 6B–6H). Of note, palmitate (200 μM, 24 h) administration in these cells resulted in increased expression of *Lbp* in parallel to increased lipogenesis (including *Srebf1*, *Scd1*, *Idh1*, and *Me1* mRNA and ACC protein and activity), oxidative stress (such as expression of *Gpx4* and *Sod2* mRNA), and ER stress (*Syvn1*, *Atf6*, and *Hspa5* mRNA) (Figures 6A–6I). Otherwise, palmitate attenuated AMPK activity (Figure 6F) and decreased metabolic activity as shown using an MTT assay (Figure 6J). Under these conditions of palmitate excess, *Lbp* gene knockdown prevented most of these negative effects, resulting in decreased lipogenesis (reducing *Srebf1*, *Scd1*, *Idh1*, and *Me1* mRNA and ACC activity but increasing AMPK activity), oxidative stress (*Gpx4* and *Sod2* mRNA), and gene-expression markers related to ER stress and improved metabolic activity (Figures 6A–6J).

Figure 4. Effect of LNP-*Lbp* UNA-siRNA treatment on insulin resistance during HFHS diet and in mice with established obesity

(A–F) Effects of 6-months LNP-*Lbp* UNA-siRNA administration on insulin at 4, 8, and 25 weeks (A), insulin change between weeks 4 and 8 (B), and fasting glucose, HOMA$_{IR}$, blood glucose during ITT, and glycemia (AUC) in ITT at the end of experiment (C–F) in HFHS-fed female and male mice. *$p < 0.05$, **$p < 0.01$, and ***$p < 0.001$ compared with CD; †$p < 0.05$ and ††$p < 0.01$ compared with HFHS; ‡$p < 0.05$, ‡‡$p < 0.01$, and ‡‡‡$p < 0.001$ compared with female mice. (G and H) Effect of 8-weeks LNP-*Lbp* UNA-siRNA administration on blood glucose during ITT (G) and glycemia (AUC) in ITT (H) in obese female and male mice. *$p < 0.05$ and **$p < 0.01$ compared with obese vehicle; ‡‡$p < 0.01$ and ‡‡‡$p < 0.001$ compared with female mice.

Lbp gene knockdown reduced lipid accumulation in primary human hepatocytes

In primary human hepatocytes, *LBP* gene knockdown resulted in reduced intracellular lipid accumulation (Figures 7A and 7B) in parallel to decreased *SCD1* mRNA levels (Figure 7C), and increased expression of β-oxidation (*CPT1A* and *PPARA*)-related genes and AMPK activity (Figures 7D–7F). *LBP* gene knockdown did not impact on expression of inflammation (*IL6* and *IL8*)-related genes (Figures 7G and 7H).

Plasma LBP levels are associated with *de novo* lipogenic genes expression and hepatic steatosis in morbidly obese human subjects

Finally, we tested whether our observations could have translational implications in subjects with morbid obesity. Anthropometric and clinical parameters are shown in Table S1. Circulating LBP was increased in patients with non-alcoholic fatty liver disease (NAFLD)

(Figure 8A). Similar to HFHS-fed mice (Figure 1D), liver *LBP* mRNA was not associated with NAFLD (Figure 8B). Increased plasma LBP levels were found in those participants with an increased ballooning degeneration score (Table S2). Circulating LBP concentration was positively correlated with liver *LBP* (r = 0.33, p = 0.01; Figure 8C). Most importantly, liver *LBP* mRNA and plasma LBP levels were positively correlated with expression of *de novo* lipogenesis-related genes (such as *FASN*, *ACACA*, and *SREBF1*) (Figures 8D–8G).

DISCUSSION

To the best of our knowledge, the possible impact of Lbp on diet-induced liver steatosis has only been explored in the LBP KO mouse model.[14] The current study was designed to specifically inhibit Lbp in the liver of wild-type mice. Thus, this would be the first study, to our knowledge, testing the therapeutic potential of liver Lbp for fatty liver. The delivery of LNPs containing *Lbp* UNA-siRNA had a preventive
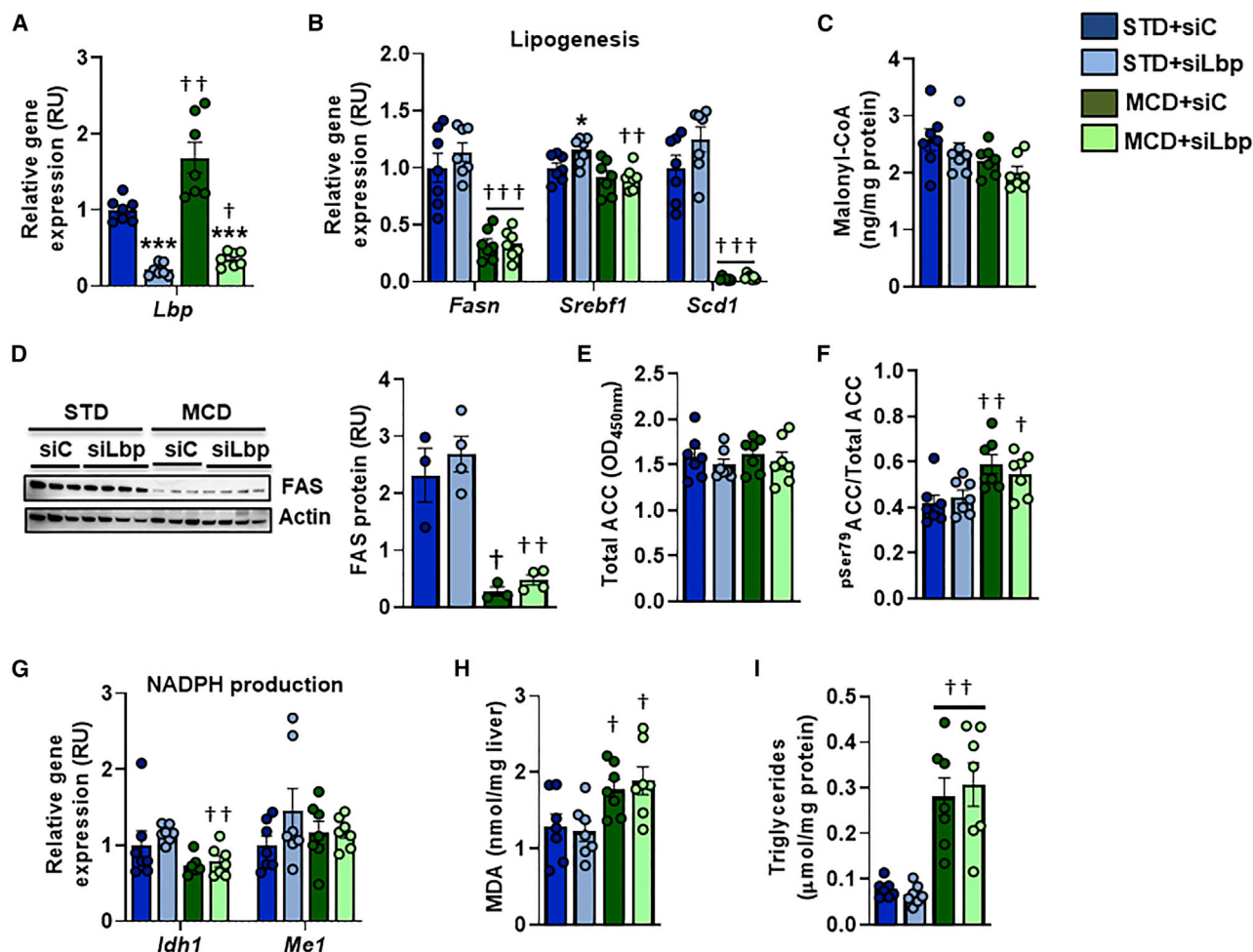
Figure 5. LNP-*Lbp* UNA-siRNA treatment effects on liver lipogenesis and triglycerides in mice fed with standard diet (STD) and MCD

(A–I) Effects of weekly LNP-*Lbp* UNA-siRNA administration in STD- and MCD-fed mice on liver *Lbp* and lipogenesis (*Fasn*, *Srebf1*, and *Scd1*)-related gene expression (A and B), malonyl-CoA (C), FAS and ACC protein levels (D and E), ACC activity (F), NADPH production (*Idh1*, *Me1*)-related gene expression (G), MDA (H), and triglycerides levels (I). $*p < 0.05$, $**p < 0.01$, and $***p < 0.001$ compared with vehicle; $^{†}p < 0.05$, $^{††}p < 0.01$, and $^{†††}p < 0.001$ compared with STD. siC, weekly LNP-non-targeting UNA-siRNA (3 mg/kg)-treated mice; siLbp, weekly LNP-*Lbp* UNA-siRNA (3 mg/kg)-treated mice.

effect on liver lipid accumulation after an HFHS diet in mice and reduced lipid accumulation in mice with established obesity. However, additional experiments in mice with established liver lipidosis should be required to further demonstrate this therapeutic effect. The consistency in the reduction of stearoyl-CoA desaturase (*Scd1*) mRNA levels in all the experimental models we used suggests that part of the beneficial effects of the treatment could be through Scd1 suppression. In fact, Scd1 is a key gene involved in triglyceride biosynthesis and upregulated in liver steatosis,[25] and targeting of *Scd1* has been shown to prevent and attenuate NAFLD progression through the inhibition of liver *de novo* lipogenesis and increased oxidative phosphorylation activity.[26–28] In agreement with current findings, the ablation of the Scd1 gene is associated with increased phosphorylation and activity of AMPK in parallel to decreased ACC activity and malonyl-CoA levels.[29]

Consistent with previous observations showing that disturbances in lipid metabolism[30,31] and oxidative stress[32,33] play an important role in MAFLD pathogenesis, we also found that markers of ROS production (MDA) associated with lipid peroxidation were significantly increased after HFHS and attenuated by LNP-*Lbp* UNA-siRNA administration. Peroxisomal oxidation of fatty acids is the most important contributor to ROS production in rat livers after HFHS[34] and in patients with increased intrahepatic fat content.[35]

A potential mechanism that would explain the beneficial effects of liver LBP depletion would be the prevention of HFHS-induced liver lipogenesis and, specially, the increased levels of Scd1. In fact, LBP depletion did not impact liver lipid accumulation in those experimental models in which liver lipogenesis/Scd1 was not triggered (standard diet) or was inhibited (MCD diet). Further confirming
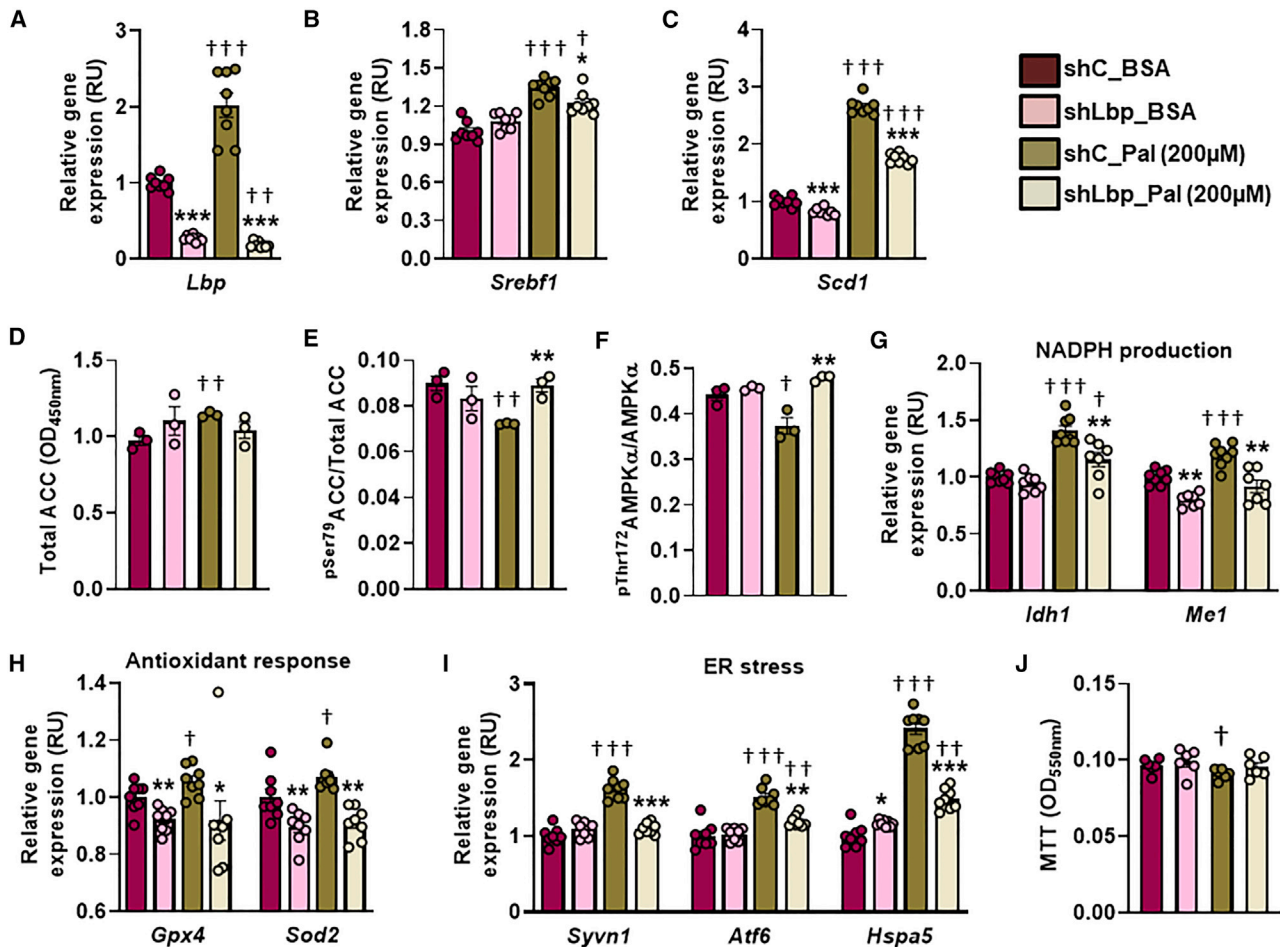
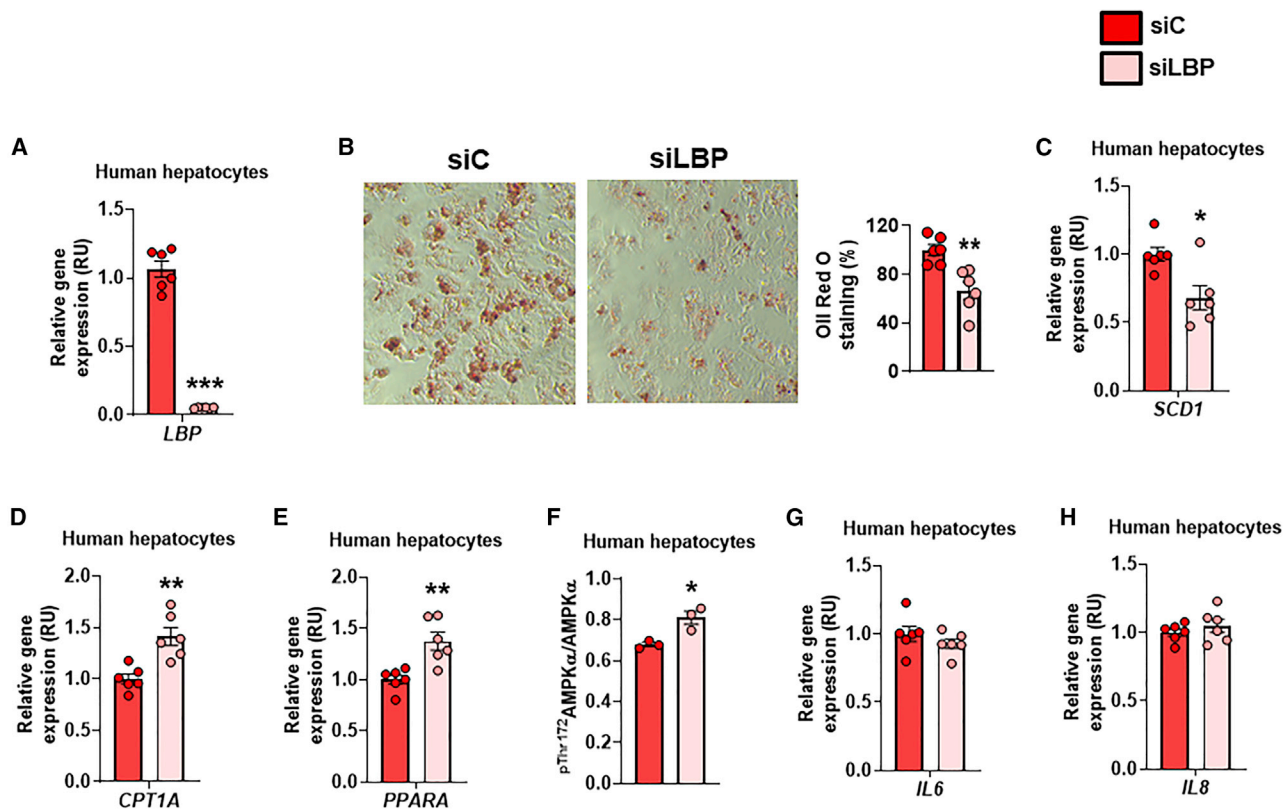**Figure 6. Impact of *Lbp* gene knockdown in Hepa1-6 cells**

(A–G) Effects of *Lbp* gene knockdown in vehicle (BSA5%, 24 h)- and palmitate-treated (200 μM, 24 h) Hepa1-6 cells on *Lbp* (A), *Srebf1* (B), and *Scd1* (C) gene expression, ACC protein (D), ACC and AMPK activity (E and F), NADPH production-, antioxidant response-, and ER stress (*Syvn1*, *Atf6* and *Hspa5*)-related gene expression (G–I), and cellular viability and activity (MTT assay) (J). *p < 0.05, **p < 0.01, and ***p < 0.001 compared with shC; †p < 0.05, ††p < 0.01, and †††p < 0.001 compared with BSA.

these findings, the association between LBP and lipogenesis was observed in the livers from subjects with morbid obesity.

A major challenge for using LNPs as a therapeutic delivery system is the potential induction of liver damage and undesired stimulation of immune response.[36] However, the approval of the first LNP-based siRNA therapeutic, patisiran, and more recently the LNP-mRNA based coronavirus 2019 (COVID-19) vaccine Comirnaty supports the potential of our approach as a treatment in humans.[37] We have previously shown that the chemical properties of the LUNAR system make it a successful, safe, and potent siRNA delivery system.[18] Here, we demonstrated that long-term treatment (6 months) with repeated LNP-*Lbp* UNA-siRNA weekly doses was well tolerated by the mouse liver and did not have any impact on serum ALT levels or liver fibrosis score, supporting the safety of this siRNA delivery system.

Since liver lipid accumulation is considered an important contributor to obesity-associated hepatic insulin resistance,[4] the potential therapeutic effects of LNP-*Lbp* UNA-siRNA might be extended to improve insulin action. In fact, we found that LNP-*Lbp* UNA-siRNA also resulted in a slight, but significant, decrease of glycemia during ITT and HOMA$_{IR}$, indicating positive effects improving insulin action, mainly in male mice, possibly as consequence of the reduction of liver lipid accumulation. In agreement with these findings, a recent study demonstrated that the inhibition of circulating and liver LBP in non-obese mice fed with chow standard diet resulted in improved glucose levels and glucose tolerance.[38] The effects of a high-fat diet or in obese mice were not evaluated in this latter study. Male mice were more sensitive to HFHS-associated metabolic disturbances, showing insulin resistance as soon as week 8. LNP-*Lbp* UNA-siRNA administration resulted in significant metabolic benefits, reducing hyperinsulinemia, improving insulin action, and decreasing liver lipid

Figure 7. Impact of *Lbp* gene knockdown in primary human hepatocytes

(A–H) Effects of *Lbp* gene knockdown in human hepatocytes on *Lbp* mRNA (A), oil red O staining (B), and expression of *Scd1*, *CPT1A*, *PPARA*, *IL6*, and *IL8* genes and AMPK activity (C–H). *p < 0.05, **p < 0.01, and ***p < 0.001 compared with siC. siC, control scramble siRNA.

accumulation in male mice but not in those with a metabolic healthy phenotype (females).

Taking into account other liver parameters, while LNP-*Lbp* UNA-siRNA administration for 8 weeks led to a non-significant decrease in fibrosis score, long-term (6 months) LNP-*Lbp* UNA-siRNA administration did not modify the fibrosis score compared with untreated mice fed with the same obesogenic (HFHS) diet. In addition, while LNP-*Lbp* UNA-siRNA administration for 8 weeks or 6 months in HFHS-fed mice decreased liver lipid accumulation, this intervention did not impact on the expression of liver damage and inflammation-related genes. These data suggest a disconnection between liver lipid accumulation and fibrosis/inflammation, which might be explained by the induction of lipophagy.[39] Data from *in vitro* experiments in human hepatocytes suggest that findings from HFHS-fed mice might be translated to humans. Specifically, we found that *LBP* gene knockdown in primary human hepatocytes attenuated intracellular lipid accumulation in parallel to decreased *SCD1* gene expression, and increased expression of β-oxidation-related genes and AMPK activity, without significant effects on proinflammatory cytokines.

It is important to note that the inhibition of liver LBP biosynthesis might increase the susceptibility to bacterial infection.[40–42] For this reason, a precise control of LBP depletion is required. The current study demonstrates a reversible treatment, which allows a precise modulation with controlled amounts of dosing, to inhibit transient LBP production in those situations in which this protein could have a negative impact on health, such as in obesity.[8–14]

To sum up, altogether current results substantiated the importance of liver *Lbp* gene knockdown through LNPs in the prevention and therapy of obesity-associated fatty liver, impacting on lipogenesis and constituting a potential target for MAFLD therapy.

MATERIALS AND METHODS

In vitro experiments for Lbp siRNA selection

Silencer Select Pre-designed siRNA assays si69107, si69108 and si69109 targeting mouse *Lbp* mRNA were purchased from Ambion (Life Technologies). Those same siRNA sequences were chemically modified by introducing 2′-O-methyl RNA bases, phosphorothioate linkages, and UNA to generate UNA siRNA (Integrated DNA Technologies, Coralville, IA, USA). siRNA sequences and chemical modifications are detailed in Table S3. Hepa1-6 cells were seeded on 96-well plates the day before transfection at a density of 10^4 cells per well. Following vendor recommended protocol, Lipofectamine RNAiMax was used to transfect siRNAs at different concentrations.
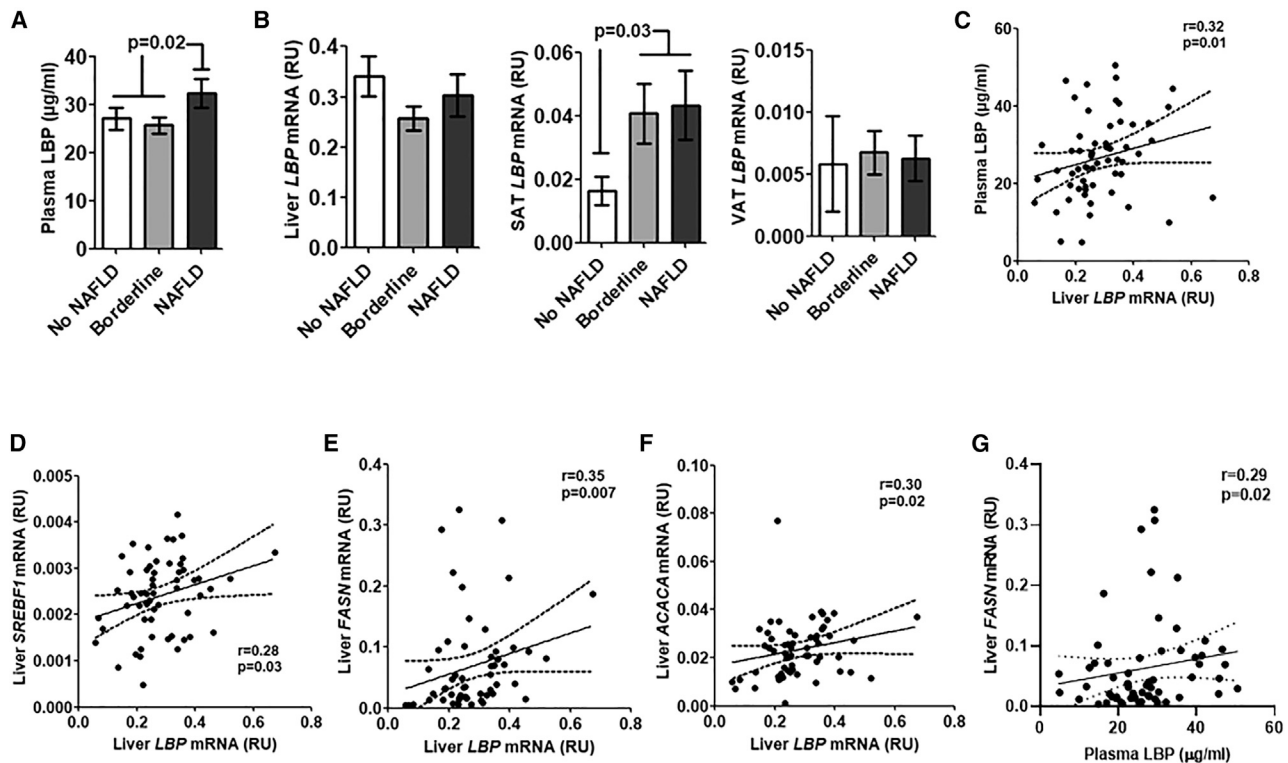
Figure 8. Association of liver *LBP* with expression of *de novo* lipogenesis genes in morbidly obese human subjects

(A and B) Plasma LBP concentration (A) and liver, SAT, and VAT *LBP* mRNA levels (B) according to NAFLD. (C) Bivariate correlations between liver *LBP* mRNA levels and plasma LBP concentration in morbidly obese participants. (D–F) Bivariate correlations between liver *LBP* and *SREBF1* (D), *FASN* (E), and *ACACA* (F) mRNA levels. (G) Bivariate correlations between plasma LBP concentration and liver *FASN* mRNA levels.

After 48 h, cells were washed with PBS, and EZCt Cells2Ct Direct Lysis Buffer (Lifeome, Oceanside, CA, USA) was added following the manufacturer's suggested protocol.

Preparation of LUNAR-*Lbp* UNA-siRNA
Using LUNAR technology, a proprietary lipid enabled nucleic acid delivery platform, Arcturus Therapeutics (San Diego, CA, USA) produced LUNAR particles encapsulating *Lbp*-UNA siRNA as described previously.[18] LUNAR is composed of four lipid components: Proprietary Arcturus Therapeutics's lipid (ATX), cholesterol, a phospholipid 1,2-distearoyl-sn-glycero-3-phosphocholine (DSPC), and a pegylated lipid. The ATX lipid contains an ionizable amino head group and a biodegradable lipid backbone. The ionizable amino head group provides the lipid with a pKa of <7. At acidic pH, the amino group is protonated and interacts with the negatively charged RNA, thus forming nanoparticles and encapsulating the RNA. However, at physiological pH, which is above the pKa of the amino head group, LUNAR nanoparticles stand neutral charge, attenuating the toxicity commonly observed with positively charged cationic transfection vectors. The pH sensitivity of the amino head group also enables protonation of the lipid once inside the endosomes, thereby promoting their interaction with the oppositely charged anionic endosomal lipids, causing destabilization of the endosomal membrane and release of RNA

payload into the cytosol. In addition, ester groups, incorporated into the lipidic backbone of ATX lipids, produce ester bonds that have good chemical stability at physiological pH but can be easily cleaved by esterases inside tissue and intracellular compartments once the load has been delivered. Finally, the remnant hydrophilic cleavage products can be quickly metabolized. Briefly, UNA siRNA was dissolved in 2 mM citrate buffer (pH 3.5). Lipids at the desired molar ratio were dissolved in ethanol. The molar ratio of the constituent lipids is 58% ATX (proprietary ionizable amino lipid), 7% DSPC (Avanti Polar Lipids, Alabaster, AL, USA), 33.5% cholesterol (Avanti Polar Lipids, Alabaster, AL, USA), and 1.5% DMG-PEG (1,2-Dimyristoyl-sn-glycerol, methoxypolyethylene glycol, PEG chain molecular weight: 2,000) (NOF America, White Plains, NY, USA). Lipid solution was then combined with UNA siRNA solution using a Nanoassemblr microfluidic device (Precision NanoSystems, Vancouver, BC, Canada) at a flow rate ratio of 1:3 ethanol:aqueous phases. The mixed material was then diluted with 3× volume of 10 mM Tris buffer (pH 7.4) containing 9% sucrose, reducing the ethanol content to 6.25%. The diluted formulation was then concentrated by tangential flow filtration using hollow fiber membranes (mPES Kros membranes, 100 Kd MWCO, Spectrum Laboratories, Rancho Dominguez, CA, USA), followed by diafiltration against 10 volumes of 10 mM Tris buffer (pH 7.4) containing 9% sucrose. Post diafiltration, formulations were then concentrated to

desired UNA-siRNA concentration, followed by filling into vials and freezing. Formulations were characterized for particle size, UNA-siRNA content, and encapsulation efficiency, as detailed in Table S4. Particle size was determined by dynamic light scattering (ZEN3600, Malvern Instruments). Encapsulation efficiency was calculated by determining unencapsulated UNA-siRNA content by measuring the fluorescence upon the addition of RiboGreen (Molecular Probes) to the particles (Fi) and comparing this value with the total RNA content that is obtained upon lysis of the particles by 1% Triton X-100 (Ft), where the percentage of encapsulation = (Ft − Fi)/Ft × 100.

Mice experiments

Pilot experiment

Eight-week-old male C57/BL6J mice (n = 25) were housed for 2 weeks under standard conditions of light (12-h light/12-h dark cycle) and temperature (22°C ± 1°C). Next, one intravenous injection into the tail of the following treatments was performed: (1) vehicle (PBS), (2–3) chemically unmodified (1 and 3 mg/kg), and (4–5) UNA-containing chemically modified (1 and 3 mg/kg) *Lbp* siRNA complexed by LUNAR delivery platform. The effect of this injection was evaluated at day 3, 6, 10, and 12, and blood was collected in citrate tubes for preparation of plasma each day. The weight of mice was measured at 8 (day −14 of injection) and 10 (day 0 of injections) weeks and 12 days after injections. Finally, at week 12, in the same mice, a second injection was performed, and 3 days later, mice were killed by suffocation under sedation, and liver was removed, immediately frozen in liquid nitrogen, and stored at −80°C until processing for RNA extraction.

Metabolic experiment

Eight-week-old male and female C57/BL6J mice (n = 46) were housed for 25 weeks under standard conditions of light (12-h light/12-h dark cycle) and temperature (22°C ± 1°C) in the following experimental conditions: (1) non-treated, CD-fed mice (TD.120455, 3.3 Kcal/g, ENVIGO) for 25 weeks; (2) non-treated, HFHS diet-fed mice (HFHS/obese vehicle; TD.08811, 4.7 Kcal/g, ENVIGO) for 25 weeks; (3) weekly LUNAR-*Lbp* UNA-siRNA-treated (3 mg/kg), HFHS-fed mice for 25 weeks (HFHS + siLbp); and (4) weekly LUNAR-*Lbp* UNA-siRNA-treated (3 mg/kg), HFHS-fed mice only in the last 8 weeks (obese + siLbp) (Figures S1A–S1D). To discriminate off-target effects from the carrier (LNPs), mice from the non-treated experimental conditions (1–2 or 4 in the first 16 weeks) were injected weekly with the corresponding buffer as the vehicle. Body weight was reported weekly. Serum and plasma were collected at 4 and 8 weeks. ITT was performed at week 20. Briefly, insulin (Actrapid; Novo Nordisk Pharma A/S, Bagsvaerd, Denmark) in saline solution was administered intraperitoneally (0.75 UI/kg) to mice, and glycemia in blood obtained from the tail was measured 15, 30, 45, 60, and 90 min after glucose injection. At week 25, after overnight fasting, mice were sacrificed by suffocation under sedation. Then, blood serum and plasma, liver, inguinal WAT (iWAT), and perigonadal WAT (pgWAT) were collected, immediately frozen in liquid nitrogen, and stored at −80°C until processing for RNA or protein analysis. A piece of liver was also fixed with 4% formalin for 24 h and then stored in 70% ethanol at 4°C for histological analysis.

In all mice experiments, the research was conducted in accordance with the European Guidelines for the Care and Use of Laboratory Animals (directive 2010/63/EU). In pilot and metabolic experiments, animal protocols were approved by the Ethical Committee for Animal Experimentation of Barcelona Science Park (PCB) and the University of Barcelona (experimental project approval number: 9955).

Standard control and MCD experiment

Eight-week-old male C57BL/6J mice (n = 28) were kept under 12-h light/12-h dark cycle and had *ad libitum* access to standard diet or MCD diet (A02082002BR, Research Diets) for 6 weeks. In the study, mice received weekly intravenous injections of non-targeting control siRNA (siRNA control) or siRNA-Lbp (3 mg/kg) for 6 weeks, and we also used the corresponding buffer as the vehicle to discriminate off-target effects from the non-targeting control siRNA (Figure S5). Sequence and validation of this non-silencing control siRNA with the same LUNAR formulation was previously reported.[43] Food intake and body weight were monitored weekly. In these experiments, animal protocols were approved by the Ethical Committee for Animal Experimentation of the University of Santiago de Compostela.

Lentiviral shRNA-Lbp particles production

Four different shLbp (clone set against mouse Lbp, NM_008489.2) primer sequences and random negative control (NC) sequences that did not have targets for any gene were synthesized by Tebu-bio (Tebu-bio, Spain, SL). Lentivirus-targeted Lbp was obtained by co-transfection of shRNA plasmids against Lbp and a combination of packaging and envelope plasmid from Addgene (pCMV-VSV-G and pCMV-dR8.2 dvpr) into HEK293T using LipoD293 transfection reagent following manufacturers' instructions. shRNA sequence for knockdown Lbp gene is detailed in Table S3. Obtained lentiviruses were used to treat Hepa1-6 cell line. Lentivirus effectiveness was confirmed in Hepa1-6 cells.

In vitro experiments with lentiviral shRNA-Lbp particles

The mouse hepatoma Hepa1-6 cell line was purchased from American Type Culture Collection (ATCC, Manassas, VA, USA) and cultured in Dulbecco's modified Eagle's medium (DMEM) supplemented with 4,500 mg/L glucose, 10% fetal bovine serum (Gibco), 100 units/mL penicillin and streptomycin, 1% glutamine, and 1% sodium pyruvate, at 37 °C and 5% CO_2 atmosphere. Gene silencing was achieved using *Lbp*-targeted and control shRNA lentiviral particles. Stable clones expressing the shRNA were selected by puromycin dihydrochloride. Treatments were performed in Hepa1-6 for 24 h after seeding. Fatty acid accumulation was induced by palmitate exposure as follows: 27.84 mg of palmitate (Sigma, St. Louis, MO, USA) were dissolved in 1 mL sterile water to make a 100 mM stock solution. An aliquot of 5% BSA was prepared in serum-free DMEM. One-hundred mM palmitate stock solution and 5% BSA were mixed for at least 1 h at 40°C to obtain a 5 mM solution. Hepa1-6 cells were treated with 0.2 mM palmitate for 24 h. BSA-supplemented medium was used as vehicle. Four biological replicates were collected from 2 independent experiments.

In vitro experiments in primary human hepatocytes

Commercially available (Innoprot, Bizkaia, Spain) primary human hepatocytes (HHs) were cultured with hepatocyte medium (Innoprot) supplemented with 5% fetal bovine serum (FBS), 1% hepatocyte growth supplement (i.e., an optimized combination of growth factors, hormones, and proteins required for primary hepatocyte cultures), and 100 units/mL penicillin and streptomycin (P/S). HHs were grown on fibronectin pre-coated dishes at 37°C and 5% CO_2 atmosphere. Twenty-four h after seeding, HHs were forward transfected with siRNAs for 72 h. Briefly, the siRNA (Sigma-Aldrich, St. Louis, MO, USA) against LBP and Lipofectamine RNAiMAX (Life Technologies, Darmstadt, Germany) were diluted separately with Opti-MEM I Reduced Serum Medium (Life Technologies, Darmstadt, Germany) and mixed by pipetting afterward. The siRNA-RNAiMAX complexes were left to incubate for 20 min at room temperature and subsequently added on the top of the adherent cells drop-wise. The final concentrations of Lipofectamine RNAiMAX and esiRNAs were 1.6 μL/cm^2 and 75 nM, respectively, in 24-well cell culture plates, and the final amount of medium per well was 1 mL. Hepatocytes were harvested 72 h after transfection without changing cell culture medium. Transfection efficiency was assessed by real-time PCR. The siRNAs (Sigma-Aldrich) used were human LBP (SA-SI_HS02_0033699) and the MISSION siRNA Universal Negative Control #1 (Sigma-Aldrich, SIC001) as non-targeting siRNA. For quantification of lipid droplets, at the end of the experiment, HHs were fixed with paraformaldehyde 4% for 1 h. Cells were dipped in 60% isopropanol before they were dried and stained with oil red O (Sigma-Aldrich, St. Louis, MO, USA) for 10 min at room temperature. Pictures were taken using Nikon Eclipse Ts2 inverted microscope (100× total magnification). Absorbance was measured at 500 nm. All experimental conditions were tested in 6 biological replicates.

Gene-expression analysis

RNA purification (isolation) was performed using the RNeasy Lipid Tissue Mini Kit (QIAgen, Izasa SA, Barcelona, Spain), and the integrity was checked by the Agilent Bioanalyzer (Agilent Technologies, Palo Alto, CA, USA). Gene expression was assessed by real-time PCR using a LightCycler 480 Real-Time PCR System (Roche Diagnostics SL, Barcelona, Spain), using TaqMan technology suitable for relative genetic expression quantification. The commercially available and pre-validated TaqMan primer/probe sets (Thermo Fisher Scientific, Waltham, MA, USA) used were as follows: endogenous control 18S and target gene mouse LBP (Lbp; Mm00493139_m1); fatty acid synthase (Fasn; Mm00662319_m1); stearoyl-CoA desaturase 1 (Scd1; Mm00772290_m1); acetyl-CoA carboxylase alpha (Acaca; Mm01304257_m1); sterol regulatory element binding transcription factor 1 (Srebf1; Mm00550338_m1); isocitrate dehydrogenase 1 (NADP+), soluble (Idh1; Mm00516030_m1); malic enzyme 1, NADP(+)-dependent, cytosolic (Me1; Mm00782380_s1); glutathione S-transferase, alpha 3 (Gsta3; Mm00494798_m1); glutathione peroxidase 4 (Gpx4; Mm00515041_m1); superoxide dismutase 2, mitochondrial (Sod2; Mm01313000_m1); synovial apoptosis inhibitor 1, synoviolin (Syvn1; Mm00511995_m1); activating transcription factor 6 (Atf6; Mm01295316_m1); and heat shock protein 5 (Hspa5; Mm00517691_m1). In humans, peptidylprolyl isomerase A (cyclophilin A) (4333763, PPIA as endogenous control); LBP (LBP; Hs01084621_m1); fatty acid synthase (FASN; Hs00188012_m1); acetyl-CoA carboxylase alpha (ACACA; Hs01046047_m1); sterol regulatory element binding transcription factor 1 (SREBF1; Hs02561944_s1); stearoyl-CoA desaturase (SCD1; Hs01682761_m1); peroxisome proliferator activated receptor alpha (PPARA; Hs00947536_m1); carnitine palmitoyltransferase 1A (CPT1A; Hs00912671_m1); interleukin-6 (IL-6; Hs00985639_m1); and C-X-C motif chemokine ligand 8 (CXCL8 or IL-8; Hs00174103_m1) were used.

The information of all primer/probe sets used is available on the Thermo Fisher Scientific website and can be obtained using the assay reference for each gene.

Histological procedures

Masson's trichrome staining

Tissue processing and a standard Masson's trichrome staining was performed at Allele Biotechnologies (San Diego, CA, USA). After stain, slides were examined by a certified pathologist at HistoTox Labs (Boulder, CO, USA), who evaluated and quantified the degree of fibrosis. LD area and number were assessed using Fiji (NIH).[44] A minimum of four random regions of interest (ROIs) of 151.719 μm^2 were created from each image, and the area and number of the LDs contained in the ROI was retrieved and analyzed.

Quantification of triglycerides in liver

Liver (∼20 mg) samples were homogenized using a TissueLyser LT in 400 μL of distilled water containing 5% Igepal CA-630, boiled for 5 min twice, and centrifuged at 13,000 × g for 5 min. Triglycerides were measured in the supernatant, which was diluted 10-fold with water before assay, using the Triglyceride Quantification Kit (MAK266; Merck Life Science, Madrid, Spain) and strictly following the manufacture's protocol.

Malonyl-CoA measurement

Liver (∼20 mg) was homogenized in PBS and centrifuged for 20 min at 2,000–3,000 RPM, and supernatant was used to measure malonyl-CoA levels using Mouse Malonyl-CoA ELISA KIT (cat. no. EK18900, Signalway Antibody, Greenbelt, MD, USA) and strictly following the manufacture's protocol.

ACC and AMPKα activity

ACC and AMPKα activities were inferred through the ratio of phosphorylation in serine 79 for ACC (^{pSer79}ACC) and in threonine 172 for AMPKα (^{pThr172}AMPKα) versus total ACC and AMPKα protein amount, respectively. Increased ^{pSer79}ACC/total ACC indicates decreased ACC activity, whereas increased ^{pThr172}AMPKα/AMPKα is proportional to AMPKα activity. ^{pSer79}ACC, total ACC, ^{pThr172}AMPKα, and AMPKα were measured by PathScan Phospho-Acetyl-CoA Carboxylase (Ser79) Sandwich ELISA Kit (#7986C); PathScan Total Acetyl-CoA Carboxylase Sandwich ELISA Kit (#7996C); PathScan Phospho-AMPKα (Thr172) Sandwich ELISA Kit (#7959C); and PathScan total

AMPKα Sandwich ELISA Kit (#7961C, Cell Signaling, Danvers, MA, USA). Liver (~30 mg) and Hepa1-6 cells (~3.5×10^5 cells) were homogenized in PathScan Sandwich ELISA Lysis Buffer ($1\times$) containing phenylmethylsulfonyl fluoride (0.2 mM, P7626, Merck Life Science, Madrid, Spain). Tissue lysates were centrifuged at $1,500 \times g$ for 5 min at $4°C$ to remove tissue and cell debris, protein content was quantified using the Lowry method, and tissue and cell lysates were diluted at the same recommended protein concentration (0.3 mg/mL for total ACC and AMPKα and 1 mg/mL for phosphorylated ACC and AMPKα). Test procedure performed following the manufacture's protocol.

Western blot analysis

Liver (30 mg) was homogenized in lysis cell buffer (50 mmol/L Tris-HCl [pH 7.4], 150 mmol/L NaCl, 1.5 mmol/L $MgCl_2$, 1 mmol/L EDTA, 1 mmol/L EGTA, 40 mmol/L β-glycerophosphate, 2 mmol/L Na_3VO_4, 1 mmol/L PMSF, 1 mmol/L DTT) containing complete protease inhibitor cocktail (Roche Applied Science). Tissue lysates were centrifuged at $1,500 \times g$ for 5 min at $4°C$ to remove cell debris, and protein content was quantified using the Lowry method. For western blotting, proteins (40 µg) were resolved by SDS-PAGE and transferred to a PVDF membrane (Immobilon; Millipore). Membranes were exposed overnight at $4°C$ to primary antibodies anti-fatty acid synthase (FAS [C20G5], rabbit monoclonal antibody [mAb] #3180) at 1/1,000 dilution (Cell Signaling, Danvers, MA, USA) and anti-β-actin at 1/1,000 (sc-47778, Santa Cruz Biotechnology, Dallas, TX, USA) both diluted in $1\times$ PBS containing 0.1% Tween 20, following the recommendations of the manufacturer. After secondary antibody incubation (anti- mouse/rabbit HRP), signals were detected using enhanced chemiluminescence HRP substrate (Millipore) and analyzed with a luminescent image analyzer ChemiDoc MP Imaging System (Bio-Rad, Hercules, CA, USA).

MDA measurement

Liver MDA levels were measured by Lipid Peroxidation (MDA) Assay Kit (cat. no. MAK085, Merck Life Science, Madrid, Spain), with liver (~20 mg) samples processed and assayed strictly following the manufacture's protocol.

Human study

Fifty-eight morbidly obese subjects were recruited from the ongoing multicenter FLORINASH Project. Participants were recruited at the Endocrinology Service of the Hospital Universitari Dr. Josep Trueta (Girona, Spain). Anthropometric and clinical parameters are described in Table S1. Inclusion criteria were age 30 to 65 years and ability to understand study procedures. Exclusion criteria were systemic diseases, infection in the previous month, serious chronic illness, >20 g ethanol intake/day, or use of medications that might interfere with insulin action. Liver and subcutaneous and adipose tissue (SAT and VAT, respectively) tissue samples were collected and snap frozen in liquid nitrogen for gene-expression analysis. Liver samples were also fixed in formalin for the histological assessment. Fixed samples were stained with hematoxylin and eosin and Masson's trichrome stain. All samples were evaluated by the same pathologist according to the degree of steatosis. Then, participants were stratified as subjects without significant steatosis (<5%), "borderline" (5%–33%), and subjects with significant steatosis (>33% of fat). Additional exclusion criteria in this subgroup of participants included cirrhosis or bridging fibrosis, a liver biopsy less than 2-cm long, and the use of statins. This study was carried out in accordance with the recommendations of the ethical committee of the Hospital of Girona Dr. Josep Trueta. The protocol was approved by the ethical committee of the Hospital of Girona Dr. Josep Trueta (approval number: 27052013). All subjects gave written informed consent in accordance with the Declaration of Helsinki after the purpose of the study was explained to them.

Serum/plasma measurements

Plasma LBP (HK205-02, LBP mouse ELISA kit, Hycult Biotech, Plymouth Meeting, PA, USA), insulin (90080, Crystal Chem, Zaandam, the Netherlands), glucose (Accutrend; Roche Diagnostics, Mannheim, Germany), and ALT activity (Alfa Wasserman/Vet Axcel Reagent SA1046) were measured using commercial kits according to manufacturer's instructions.

In human study, plasma LBP was measured by human LBP enzyme-linked immunosorbent assay (ELISA) kit (HK315-02, HyCult Biotechnology, Huden, the Netherlands) with intra- and interassay coefficients of variation <8%. Serum glucose levels were measured in duplicate by the glucose oxidase method with a Beckman Glucose Analyzer 2 (Beckman Instruments, Brea, CA, USA). The coefficient of variation (CV) was 1.9%. Total serum cholesterol was measured through the reaction of cholesterol esterase/oxidase/peroxidase, using a BM/Hitachi 747. HDL cholesterol was quantified after precipitation with polyethylene glycol at room temperature. Total serum triglycerides were measured through the reaction of glycerol-phosphate-oxidase and peroxidase by routine laboratory tests on a Hitachi 917 instrument (Roche, Mannheim, Germany). Glycosylated hemoglobin (HbA_{1c}) was measured by the high-performance liquid chromatography method (Bio-Rad, Muenchen, Germany, and autoanalyzer Jokoh HS-10, respectively). Intra- and interassay CVs were <4% for all these tests. C-reactive protein (ultrasensitive assay; 110 Beckman, Fullerton, CA, USA) was determined by a routine laboratory test.

Statistical analysis

Statistical analyses were performed using the SPSS 12.0 software. In human study, unless otherwise stated, descriptive results of continuous variables are expressed as mean and SD for Gaussian variables or median and interquartile range for non-Gaussian variables. The relation between variables was analyzed by simple correlation (using Spearman's and Pearson's tests). One-factor ANOVA was used to compare clinical variables and liver *LBP* gene expression relative to parameters related to liver pathology. In mice experiments, all results are expressed as means ± SEM, and differences were tested for statistical significance using Student's unpaired and paired t tests and non-parametric tests (Mann-Whitney U test). Levels of statistical significance were set at $p < 0.05$.

Data availability statement

All data generated or analyzed during this study are included in this published article (and its supplemental information).

SUPPLEMENTAL INFORMATION

Supplemental information can be found online at https://doi.org/10.1016/j.omtn.2022.08.003.

AUTHOR CONTRIBUTIONS

R.D.-T., M.G., J.M.F.-R., and J.M.M.-N. participated in study design and analysis of data. J.L., R.D.-T., F.C., A.G.-N., E.M., N.D., S.M.-R., R.M., F.O., A.C.-N., N.O.-C., P.P.K., and J.M.M.-N. participated in acquisition of data. J.L., R.D.-T., A.G.-N., E.M., N.D., W.R., K.T., P.C., F.V., M.L., M.G., J.M.F.-R., and J.M.M.-N. participated in interpretation of data. R.D.-T. and J.M.M.-N. wrote and edited the manuscript. M.L., K.T., F.V., M.G., and J.M.F.-R. revised the manuscript critically for important intellectual content. All authors participated in final approval of the version to be published.

DECLARATION OF INTERESTS

R.D.-T., R.M., P.P.K., K.T., and P.C. are employees of Arcturus Therapeutics. The authors declared no additional conflict of interest.

REFERENCES

1. Gluchowski, N.L., Becuwe, M., Walther, T.C., and Farese, R.V. (2017). Lipid droplets and liver disease: from basic biology to clinical implications. Nat. Rev. Gastroenterol. Hepatol. 14, 343–355.

2. Taylor, R., Al-Mrabeh, A., and Sattar, N. (2019). Understanding the mechanisms of reversal of type 2 diabetes. Lancet Diabetes Endocrinol. 7, 726–736.

3. Heymsfield, S.B., and Wadden, T.A. (2017). Mechanisms, pathophysiology, and management of obesity. N. Engl. J. Med. 376, 254–266.

4. Al-Mrabeh, A., Zhyzhneuskaya, S.V., Peters, C., Barnes, A.C., Melhem, S., Jesuthasan, A., Aribisala, B., Hollingsworth, K.G., Lietz, G., Mathers, J.C., et al. (2020). Hepatic lipoprotein export and remission of human type 2 diabetes after weight loss. Cell Metab. 31, 233–249.e4.

5. Sun, L., Yu, Z., Ye, X., Zou, S., Li, H., Yu, D., Wu, H., Chen, Y., Dore, J., Clément, K., et al. (2010). A marker of endotoxemia is associated with obesity and related metabolic disorders in apparently healthy Chinese. Diabetes Care 33, 1925–1932. https://doi.org/10.2337/dc10-0340.

6. Moreno-Navarrete, J.M., Ortega, F., Serino, M., Luche, E., Waget, A., Pardo, G., Salvador, J., Ricart, W., Frühbeck, G., Burcelin, R., and Fernández-Real, J.M. (2012). Circulating lipopolysaccharide-binding protein (LBP) as a marker of obesity-related insulin resistance. Int. J. Obes. 36, 1442–1449.

7. Kheirandish-Gozal, L., Peris, E., Wang, Y., Tamae Kakazu, M., Khalyfa, A., Carreras, A., and Gozal, D. (2014). Lipopolysaccharide-Binding protein plasma levels in chil-dren: effects of obstructive sleep apnea and obesity. J. Clin. Endocrinol. Metab. 99, 656–663.

8. Liu, X., Lu, L., Yao, P., Ma, Y., Wang, F., Jin, Q., Ye, X., Li, H., Hu, F.B., Sun, L., and Lin, X. (2014). Lipopolysaccharide binding protein, obesity status and incidence of metabolic syndrome: a prospective study among middle-aged and older Chinese. Diabetologia 57, 1834–1841. https://doi.org/10.1007/s00125-014-3288-7.

9. Tilves, C.M., Zmuda, J.M., Kuipers, A.L., Nestlerode, C.S., Evans, R.W., Bunker, C.H., Patrick, A.L., and Miljkovic, I. (2016). Association of lipopolysaccharide-binding protein with aging-related adiposity change and prediabetes among African ancestry men. Diabetes Care 39, 385–391.

10. Nien, H.C., Sheu, J.C., Chi, Y.C., Chen, C.L., Kao, J.H., and Yang, W.S. (2018). One-year weight management lowers lipopolysaccharide-binding protein and its implication in metainflammation and liver fibrosis. PLoS One 13, e0207882. https://doi.org/10.1371/journal.pone.0207882.

11. Pang, J., Xu, W., Zhang, X., Wong, G.L.H., Chan, A.W.H., Chan, H.Y., Tse, C.H., Shu, S.S.T., Choi, P.C.L., Chan, H.L.Y., et al. (2017). Significant positive association of endotoxemia with histological severity in 237 patients with non-alcoholic fatty liver disease. Aliment. Pharmacol. Ther. 46, 175–182. https://doi.org/10.1111/apt.14119.

12. Kitabatake, H., Tanaka, N., Fujimori, N., Komatsu, M., Okubo, A., Kakegawa, K., Kimura, T., Sugiura, A., Yamazaki, T., Shibata, S., et al. (2017). Association between endotoxemia and histological features of nonalcoholic fatty liver disease. World J. Gastroenterol. 23, 712–722. https://doi.org/10.3748/wjg.v23.i4.712.

13. Nier, A., Engstler, A.J., Maier, I.B., and Bergheim, I. (2017). Markers of intestinal permeability are already altered in early stages of non-alcoholic fatty liver disease: studies in children. PLoS One 12, e0183282. https://doi.org/10.1371/journal.pone.0183282.

14. Jin, C.J., Engstler, A.J., Ziegenhardt, D., Bischoff, S.C., Trautwein, C., and Bergheim, I. (2017). Loss of lipopolysaccharide-binding protein attenuates the development of diet-induced non-alcoholic fatty liver disease in mice. J. Gastroenterol. Hepatol. 32, 708–715.

15. Moreno-Navarrete, J.M., Jové, M., Padró, T., Boada, J., Ortega, F., Ricart, W., Pamplona, R., Badimón, L., Portero-Otín, M., and Fernández-Real, J.M. (2017). Adipocyte lipopolysaccharide binding protein (LBP) is linked to a specific lipidomic signature. Obesity 25, 391–400.

16. Martin, T.R., Mathison, J.C., Tobias, P.S., Letúrcq, D.J., Moriarty, A.M., Maunder, R.J., and Ulevitch, R.J. (1992). Lipopolysaccharide binding protein enhances the responsiveness of alveolar macrophages to bacterial lipopolysaccharide. Implications for cytokine production in normal and injured lungs. J. Clin. Invest. 90, 2209–2219.

17. Moreno-Navarrete, J.M., Escoté, X., Ortega, F., Serino, M., Campbell, M., Michalski, M.C., Laville, M., Xifra, G., Luche, E., Domingo, P., et al. (2013). A role for adipocyte-derived lipopolysaccharide-binding protein in inflammation- and obesity-associated adipose tissue dysfunction. Diabetologia 56, 2524–2537. https://doi.org/10.1007/s00125-013-3015-9.

18. Ramaswamy, S., Tonnu, N., Tachikawa, K., Limphong, P., Vega, J.B., Karmali, P.P., Chivukula, P., and Verma, I.M. (2017). Systemic delivery of factor IX messenger RNA for protein replacement therapy. Proc. Natl. Acad. Sci. USA 114, E1941–E1950.

19. Stein, S., Lemos, V., Xu, P., Demagny, H., Wang, X., Ryu, D., Jimenez, V., Bosch, F., Lüscher, T.F., Oosterveer, M.H., and Schoonjans, K. (2017). Impaired SUMOylation of nuclear receptor LRH-1 promotes nonalcoholic fatty liver disease. J. Clin. Invest. 127, 583–592.

20. Busserolles, J., Mazur, A., Gueux, E., Rock, E., and Rayssiguier, Y. (2002). Metabolic syndrome in the rat: females are protected against the pro-oxidant effect of a high sucrose diet. Exp. Biol. Med. 227, 837–842.

21. Shechter, I., Dai, P., Huo, L., and Guan, G. (2003). IDH1 gene transcription is sterol regulated and activated by SREBP-1a and SREBP-2 in human hepatoma HepG2 cells: evidence that IDH1 may regulate lipogenesis in hepatic cells. J. Lipid Res. 44, 2169–2180.

22. Metallo, C.M., Gameiro, P.A., Bell, E.L., Mattaini, K.R., Yang, J., Hiller, K., Jewell, C.M., Johnson, Z.R., Irvine, D.J., Guarente, L., et al. (2011). Reductive glutamine metabolism by IDH1 mediates lipogenesis under hypoxia. Nature 481, 380–384.

23. Al-Dwairi, A., Pabona, J.M.P., Simmen, R.C.M., and Simmen, F.A. (2012). Cytosolic malic enzyme 1 (ME1) mediates high fat diet-induced adiposity, endocrine profile,

and gastrointestinal tract proliferation-associated biomarkers in male mice. PLoS One 7, e46716.

24. Rizki, G., Arnaboldi, L., Gabrielli, B., Yan, J., Lee, G.S., Ng, R.K., Turner, S.M., Badger, T.M., Pitas, R.E., and Maher, J.J. (2006). Mice fed a lipogenic methionine-choline-deficient diet develop hypermetabolism coincident with hepatic suppression of SCD-1. J. Lipid Res. 47, 2280–2290.

25. Benhammou, J.N., Ko, A., Alvarez, M., Kaikkonen, M.U., Rankin, C., Garske, K.M., Padua, D., Bhagat, Y., Kaminska, D., Kärjä, V., et al. (2019). Novel lipid long inter-vening noncoding RNA, oligodendrocyte maturation-associated long intergenic non-coding RNA, regulates the liver steatosis gene stearoyl-coenzyme A desaturase as an enhancer RNA. Hepatol. Commun. 3, 1356–1372.

26. Ntambi, J.M., Miyazaki, M., Stoehr, J.P., Lan, H., Kendziorski, C.M., Yandell, B.S., Song, Y., Cohen, P., Friedman, J.M., and Attie, A.D. (2002). Loss of stearoyl-CoA desaturase-1 function protects mice against adiposity. Proc. Natl. Acad. Sci. USA 99, 11482–11486.

27. Iruarrizaga-Lejarreta, M., Varela-Rey, M., Fernández-Ramos, D., Martínez-Arranz, I., Delgado, T.C., Simon, J., Juan, V.G.d., de la Cruz-Villar, L., Azkargorta, M., Lavin, J.L., et al. (2017). Role of aramchol in steatohepatitis and fibrosis in mice. Hepatol. Commun. 1, 911–927.

28. Safadi, R., Konikoff, F.M., Mahamid, M., Zelber-Sagi, S., Halpern, M., Gilat, T., and Oren, R.; FLORA Group (2014). The fatty acid-bile acid conjugate aramchol reduces liver fat content in patients with nonalcoholic fatty liver disease. Clin. Gastroenterol. Hepatol. 12, 2085–2091.e1.

29. Dobrzyn, P., Dobrzyn, A., Miyazaki, M., Cohen, P., Asilmaz, E., Hardie, D.G., Friedman, J.M., and Ntambi, J.M. (2004). Stearoyl-CoA desaturase 1 deficiency in-creases fatty acid oxidation by activating AMP-activated protein kinase in liver. Proc. Natl. Acad. Sci. USA 101, 6409–6414.

30. Min, H.K., Kapoor, A., Fuchs, M., Mirshahi, F., Zhou, H., Maher, J., Kellum, J., Warnick, R., Contos, M.J., and Sanyal, A.J. (2012). Increased hepatic synthesis and dysregulation of cholesterol metabolism is associated with the severity of nonalco-holic fatty liver disease. Cell Metab. 15, 665–674. https://doi.org/10.1016/j.cmet.2012.04.004.

31. Chiappini, F., Coilly, A., Kadar, H., Gual, P., Tran, A., Desterke, C., Samuel, D., Duclos-Vallée, J.C., Touboul, D., Bertrand-Michel, J., et al. (2017). Metabolism dys-regulation induces a specific lipid signature of nonalcoholic steatohepatitis in pa-tients. Sci. Rep. 7, 46658.

32. Bessone, F., Razori, M.V., and Roma, M.G. (2019). Molecular pathways of nonalco-holic fatty liver disease development and progression. Cell. Mol. Life Sci. 76, 99–128.

33. Galmés-Pascual, B.M., Martínez-Cignoni, M.R., Morán-Costoya, A., Bauza-Thorbrügge, M., Sbert-Roig, M., Valle, A., Proenza, A.M., Lladó, I., and Gianotti, M. (2020). 17B-Estradiol ameliorates lipotoxicity-induced hepatic mitochondrial oxidative stress and insulin resistance. Free Radic. Biol. Med. 150, 148–160.

34. Mamun, M.A.A., Faruk, M., Rahman, M.M., Nahar, K., Kabir, F., Alam, M.A., and Subhan, N. (2019). High carbohydrate high fat diet induced hepatic steatosis and dys-lipidemia were ameliorated by psidium guajava leaf powder supplementation in rats. Evidence-based Complement. Alternat. Med. 2019.

35. Monserrat-Mesquida, M., Quetglas-Llabrés, M., Abbate, M., Montemayor, S., Mascaró, C.M., Casares, M., Tejada, S., Abete, I., Zulet, M.A., Tur, J.A., et al. (2020). Oxidative stress and pro-inflammatory status in patients with non-alcoholic fatty liver disease. Antioxidants 9, 7599.

36. Cullis, P.R., and Hope, M.J. (2017). Lipid nanoparticle systems for enabling gene ther-apies. Mol. Ther. 25, 1467–1475.

37. Adams, D., Gonzalez-Duarte, A., O'Riordan, W.D., Yang, C.-C., Ueda, M., Kristen, A.V., Tournev, I., Schmidt, H.H., Coelho, T., Berk, J.L., et al. (2018). Patisiran, an RNAi therapeutic, for hereditary transthyretin amyloidosis. N. Engl. J. Med. 379, 11–21.

38. Molinaro, A., Koh, A., Wu, H., Schoeler, M., Faggi, M.I., Carreras, A., Hallén, A., Bäckhed, F., and Caesar, R. (2020). Hepatic expression of Lipopolysaccharide Binding Protein (Lbp) is induced by the gut microbiota through Myd88 and impairs glucose tolerance in mice independent of obesity. Mol. Metab. 37, 100997. https://doi.org/10.1016/j.molmet.2020.100997.

39. Chen, M., Liu, J., Yang, W., and Ling, W. (2017). Lipopolysaccharide mediates hepatic stellate cell activation by regulating autophagy and retinoic acid signaling. Autophagy 13, 1813–1827.

40. Knapp, S., de Vos, A.F., Florquin, S., Golenbock, D.T., and van der Poll, T. (2003). Lipopolysaccharide binding protein is an essential component of the innate immune response to Escherichia coli peritonitis in mice. Infect. Immun. 71, 6747–6753.

41. Lamping, N., Dettmer, R., Schröder, N.W., Pfeil, D., Hallatschek, W., Burger, R., and Schumann, R.R. (1998). LPS-binding protein protects mice from septic shock caused by LPS or gram-negative bacteria. J. Clin. Invest. 101, 2065–2071.

42. Zweigner, J., Gramm, H.J., Singer, O.C., Wegscheider, K., and Schumann, R.R. (2001). High concentrations of lipopolysaccharide-binding protein in serum of pa-tients with severe sepsis or septic shock inhibit the lipopolysaccharide response in hu-man monocytes. Blood 98, 3800–3808.

43. Yanagi, T., Tachikawa, K., Wilkie-Grantham, R., Hishiki, A., Nagai, K., Toyonaga, E., Chivukula, P., and Matsuzawa, S.I. (2016). Lipid nanoparticle-mediated siRNA trans-fer against PCTAIRE1/PCTK1/cdk16 inhibits in vivo cancer growth. Mol. Ther. Nucleic Acids 5, e327.

44. Zazo Seco, C., Castells-Nobau, A., Joo, S.H., Schraders, M., Foo, J.N., Van Der Voet, M., Velan, S.S., Nijhof, B., Oostrik, J., de Vrieze, E., et al. (2017). A homozygous FITM2 mutation causes a deafness-dystonia syndrome with motor regression and signs of ichthyosis and sensory neuropathy. Dis. Model. Mech. 10, 105–118.